Birth of strange nonchaotic attractors in a piecewise linear oscillator

Jicheng Duan[a], Wei Zhou[a,b], [1] Denghui Li[c], Celso Grebogi[d]

[a]*School of Mathematics and Physics, Lanzhou Jiaotong University, Lanzhou, Gansu 730070, China*
[b]*Institute of Decision and Game Theory, Lanzhou Jiaotong University, Lanzhou, Gansu 730070, China*
[c]*School of Mathematics and Statistics, Hexi University, Zhangye, Gansu 734000, China*
[d]*Institute for Complex Systems and Mathematical Biology King's College, University of Aberdeen, Aberdeen AB24 3UE, United Kingdom*

Abstract

The nonsmooth systems are widely encountered in engineering fields. They have abundant dynamical phenomena, including some results about the complex dynamics in such systems under quasiperiodic forced excitations. In this work, we consider a quasiperiodically forced piecewise linear oscillator, and show that strange nonchaotic attractors (SNAs) do exist in such nonsmooth system. The generation and evolution mechanisms of SNAs are discussed. The torus-doubling, fractal, bubbling, and intermittency routes to SNAs are identified. The strange properties of SNAs are characterized with the aid of the phase sensitivity function, singular continuous spectrum, rational frequency approximation, and the path of the partial Fourier sum of state variables in complex plane. The nonchaotic properties of SNAs are verified by the methods of maximum Lyapunov exponent and power spectrum.

Keywords: Piecewise linear oscillator, Fractalization, Strange nonchaotic attractor, Quasiperiodic excitation, Torus-doubling bifurcation.

1. Introduction

SNAs have obvious fractal geometrical structure, but the maximum Lyapunov exponent is nonpositive, which exhibits nonchaotic properties in the dynamical sense. SNAs can be regarded as a special class of attractors between quasiperiodic attractors and chaotic attractors. Since SNAs were uncovered by Grebogi et al. [1], it was realized that strangeness is not equivalent to chaos. SNAs have been widely studied in experiments and numerically. Ding et al. [2] confirmed the existence of SNAs from numerical and analytical methods, and illustrated various

[1]corresponding author. E-mail address:wei_zhou@vip.126.com (W. Zhou).

dynamical behaviors in a typical quasiperiodically forced system. Pikovsky and Feudel [3] described strange properties of such attractors by calculating the phase sensitivity exponents. With the aid of function equation for the invariant curve, Nishikawa and Kaneko [4] studied the fractal structure and chaotic evolution of a class of SNAs in a quasiperiodically forced logistic map. Ditto et al. [5] observed SNAs in a two-frequency quasiperiodically driven, buckled, magnetoelastic ribbon experiment. According to an experiment and numerical simulation, Thamilmaran et al. [6] identified chaotic attractors and SNAs in a circuit system and distinguished these two kinds of attractors by the Poincaré map, maximum Lyapunov exponents and their variance. Besides, Linder et al. [7] established the existence of strange nonchaotic star through the Kepler space telescope, which further indicates the presence of strange nonchaotic phenomena in nature.

The mathematical research of SNAs mainly focused on skew product systems, see e.g. [8–10]. Keller [11] investigated a class of skew product maps that have monotonically increasing and strictly concave fiber maps. It was proved that the system has an attracting invariant curve which is almost everywhere discontinuous and thus an SNA. Ding et al. [12] and Fuhrmann et al. [13] studied the fractal dimension of SNAs in the quasiperiodically forced monotone interval maps, which are created through nonsmooth saddle-node bifurcation, and determined that the Hausdorff dimension and box-counting dimension have different values. Other theoretical results of SNAs are about discrete Schrödinger equation with quasiperiodic potential in which the Harper map is a typical example. Haro and Puig [14] proved that the Harper map have SNAs in a set of parameter values of positive Lebesgue measure. These proofs involved spectrum analysis of the Schrödinger operator and the estimate of Lyapunov exponent.

Although the existence of SNAs has been studied widely in quasiperiodically forced systems (c.f. [15–18]), there are still many interesting questions, for instance: how did SNAs are generated and eventually evolve into chaotic attractors? Precisely, what exactly causes SNAs is somewhat vague since the bifurcation mechanisms of quasiperiodic driving systems have not been understood in detail. However, several routes to SNAs have been described in the literatures, such as Heagy-Hammel route [19, 20], fractal route [21], intermittency route [22, 23], Blowout bifurcation route [24], and so on. The literature offers overviews and further references for other routes, see e.g. [25–29].

The studies of SNAs are mainly limited to smooth systems. The mechanism of SNAs generation is more complicated in nonsmooth systems since there exist many nontypical bifurcations such as grazing bifurcation, sliding bifurcation, period-adding bifurcation, and so on. Li et al. [30] studied a piecewise smooth map quasiperiodically forced, and found three routes (Heagy-Hammel route, fractal route and type-I intermittency route) to SNAs in the parameter space. Shen and Zhang [31] revealed several types of routes to SNAs in two critical tongue-type regions in a quasiperiodically forced piecewise logistic map. Zhang et al.[32] studied a class of quasiperiodically forced interval maps, and showed that smooth quasiperiodic torus attractors lose their smoothness by grazing bifurcation and eventually become SNAs. Li et al. [33] discovered that SNAs exist between two parameter regions corresponding to chaotic motions, and further discussed the coexistence of SNAs, quasiperiodic attractors and chaotic attractors in a nonsmooth mechanical system.

The piecewise linear systems are a class of classical nonsmooth dynamical systems [34–36].

There are still only few results about the complex dynamics in such systems with quasiperiodic excitations. In this work, we identify and analyze the existence of SNAs in a piecewise linear oscillator with quasiperiodic forcing, and the dynamics transition of the system is further discussed. The remaining of this paper is organized as follows. In Section 2, we briefly describe the mathematical model of the piecewise linear oscillator and its Poincaré map. Then, the doubling and period-adding phenomena of the dynamics are investigated in Section 3. The generation and existence mechanisms of SNAs are discussed in Section 4. The main results are summarized in Section 5.

2. The piecewise linear oscillator with quasiperiodic excitation and its Poincaré map

Consider a piecewise linear oscillator shown in Fig. 1. The mass m is attached to a linear spring of stiffness k_1 and a damper of damping coefficient c_1. It is being acted upon by a quasiperiodic force $p\sin(\omega t) + \varepsilon\sin(\xi t)$. When the displacement x exceeds a certain value B, the second linear spring with stiffness k_2 contacts the mass m.

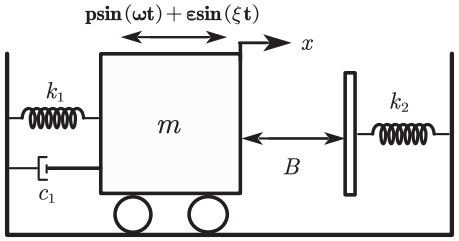

Figure 1: The piecewise linear oscillator.

The differential equation of motion of the system can be expressed as

$$m\ddot{x} + c_1\dot{x} + K(x) = p\sin(\omega t) + \varepsilon\sin(\xi t), \tag{1}$$

where

$$K(x) = \begin{cases} k_1 x, & \text{if } x \le B, \\ k_1 x + k_2(x - B), & \text{if } x > B. \end{cases} \tag{2}$$

Let $\theta = \omega t, \phi = \xi t$. Then the equation (1) can be written as the following form:

$$\begin{cases} \dot{x} = v, \\ \dot{v} = \left(-c_1 v - K(x) + p\sin(\theta) + \varepsilon\sin(\phi)\right)/m, \\ \dot{\phi} = \xi, \\ \dot{\theta} = \omega. \end{cases} \tag{3}$$

A stroboscopic section is taken in each period $2\pi/\xi$, where $\xi = (\sqrt{5} - 1)/2$. We obtain the following Poincaré map of the system (3), which has the form:

$$
\begin{aligned}
x_{n+1} &= f_1\left(x_n, v_n, \theta_n\right), \\
v_{n+1} &= f_2\left(x_n, v_n, \theta_n\right), \\
\theta_{n+1} &= \theta_n + \frac{2\pi}{\xi} \bmod 2\pi,
\end{aligned}
\tag{4}
$$

where f_1 and f_2 are determined by (3). Since ξ is the inverse of the golden ratio, the dynamics along the θ-axis is ergodic, and the trajectory for every initial condition uniformly covers the θ-axis.

3. The doubling and period-adding phenomena in the dynamics

3.1. The bifurcations in the unperturbed system

In order to understand the dynamical behavior of the system (3), we first consider the unperturbed system, i.e., the case $\varepsilon = 0$. The bifurcation diagram of the unperturbed system by varying the external excitation frequency ω is shown in Figs. 2(a) and (b), where the other parameter values are $p = 10, m = 0.5, k_1 = 1.0, k_2 = 30, c_1 = 0.2, B = 0.0001$, and the initial values are $(x_0, v_0, \theta_0, \phi_0) = (0, 0, 0, 0)$.

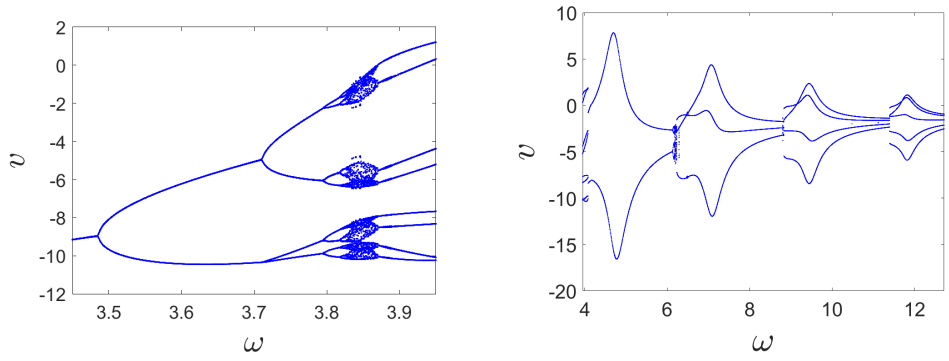

(a) (b)

Figure 2: The bifurcation diagram of the unperturbed system with respect to the parameter ω.

When the bifurcation parameter $\omega = 3.486$, the system has the first period-doubling bifurcation and the corresponding Floquet multipliers of the system are $\lambda_1 = -1$ and $\lambda_2 = -0.486$, where $\lambda_1 = -1$ goes through $(-1, 0)$ on the unit circle, and the absolute value of another eigenvalue $|\lambda_2| = 0.486 < 1$ is still inside the unit circle. As ω increases to 3.712, the system has the second period-doubling bifurcation which converts the attractor from period-2 to period-4. For $\omega = 3.797$, the period-4 attractor evolves into a period-8 attractor. When a series of period-doubling bifurcations occur, the system eventually becomes the chaotic state. When ω is greater than 3.868, the system again returns to periodic motion with a period-8 attractor. In addition, there is period-adding bifurcation in the unperturbed system, see Fig. 2(b).

3.2. The torus-doubling of the system with quasiperiodic excitation

For the system (3), we take the frequency ω as the control parameter, varying between 3.45 and 3.6. The amplitude $\varepsilon = 0.3$, the other parameter values, and the initial values are the same as in Section 3.1. The maximum Lyapunov exponent varying with the parameter ω is shown in Fig. 3, where $1\ \mathrm{T}, 2\ \mathrm{T}$ and $4\ \mathrm{T}$ correspond to torus, doubled torus, and torus of period-4 , respectively. In the system (3), SNAs do exist between quasiperiodic motion and chaotic motion. With the aid of the maximum Lyapunov exponent, we can distinguish the types of attractors in the given parameter interval. When the parameter $\omega \in [3.45, 3.562]$, the system exhibits quasiperiodic motion. When the parameter $\omega \in (3.562, 3.565)$, the system is in a strange nonchaotic state. When the parameter $\omega \in [3.565, 3.6]$, the system exhibits chaotic motion.

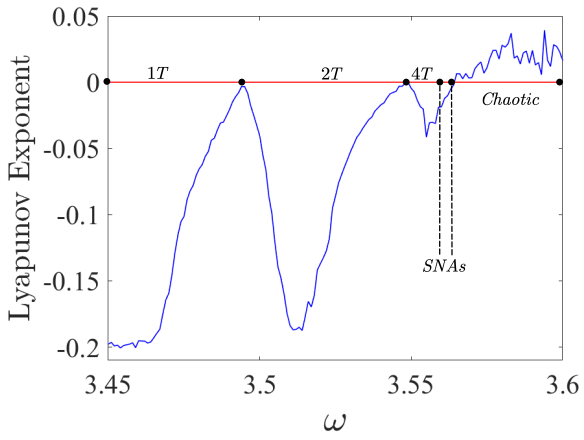

Figure 3: The maximum Lyapunov exponent with the variation of ω for the system (3).

4. Strange nonchaotic attractors

In this section, we use quantitative and qualitative methods to verify the existence of SNAs in the system (3), and describe four scenarios for the birth of the SNAs from quasiperiodic behaviors.

We first introduce the power spectrum (Fourier amplitude spectrum), which is an effective tool to distinguish various types of attractors. If the system is periodic or quasiperiodic motion, the corresponding power spectrum is purely discrete. If the system exhibits chaotic and random motion, the power spectrum is continuous. However, the SNAs behavior gives a singular continuous spectrum, which appears between discrete and continuous power spectrum (c.f. [37]). We take the Fourier transform of the process $\{x_n\}$

$$X(\Omega, T) = \sum_{n=1}^{T} x_n \mathrm{e}^{i2\pi n\Omega}. \tag{5}$$

Hence, the power spectrum of the attractor is defined as [38]

$$P_{\Omega} = \lim_{N\to\infty} |X(\Omega, T)/T|^2, \tag{6}$$

where Ω is proportional to the frequency ratio of the two excitation forces in the system.

4.1. The torus collision route

Torus collision is a generating mechanism of SNAs, which is closely related to period-doubling bifurcation. With the change of the control parameter ω, a stable 2^n T quasiperiodic attractor appears by torus-doubling bifurcation. The parent torus becomes unstable in the quasiperiodically driven system (the pitchfork bifurcation can take place in the system without driving force, that is, the unstable periodic 2^n orbit can form the periodic 2^{n+1} orbit). Hence, the stable 2^n T quasiperiodic attractor collides with its unstable parent torus to generate SNAs.

To clearly indicate the geometrically smooth or complicated structure of attractors, we can draw the phase diagrams of Poincaré section in the (θ_n, x_n)-plane with $\theta \ mod \ 2\pi$, and in (v_n, x_n)-plane, respectively. The Fig. 4 shows the evolution of typical attractors as ω varies and we can depict the creation of the SNAs by the torus-doubling. When $\omega = 3.45$, the attractor is quasiperiodic in the Poincaré sections, and the system exhibits an invariant torus in the (v_n, x_n)-plane, namely, a 1 T quasiperiodic attractor occurs, see Figs. 4(a) and (b). As ω increases, for example $\omega = 3.5$, the attractor becomes a two-tori (2T) quasiperiodic attractor and the invariant curve becomes two smooth curves, which are created by a torus-doubling bifurcation from the period-1 repellor, see Figs. 4(c) and (d). When ω passes through 3.548, the torus-doubling bifurcation occurs again, and the 2 T quasiperiodic attractor evolves into a 4 T quasiperiodic attractor, see Figs. 4(e) and (f). In general, the torus-doubling continues indefinitely until a critical point is reached beyond which the system exhibits chaotic motion. However, as ω increases further to 3.5647, the 4 T quasiperiodic attractor collides with its unstable parent torus, hence the attractor becomes extremely wrinkled, loses its smoothness and results in a strange attractor. This is reflected in Figs. 4(g) and (h) which indicate the apparent discontinuity in the Poincaré map and the doubling of the torus is interrupted. During this process, the maximum Lyapunov exponent remains negative ($\lambda \approx -0.00203$), which is shown in Fig. 3. Therefore, we conclude that the system is in the strange nonchaotic state for $\omega = 3.5647$. Finally, the attractor deforms and the SNA becomes larger and forms a chaotic attractor with $\omega = 3.567$, see Figs. 4(i) and (j).

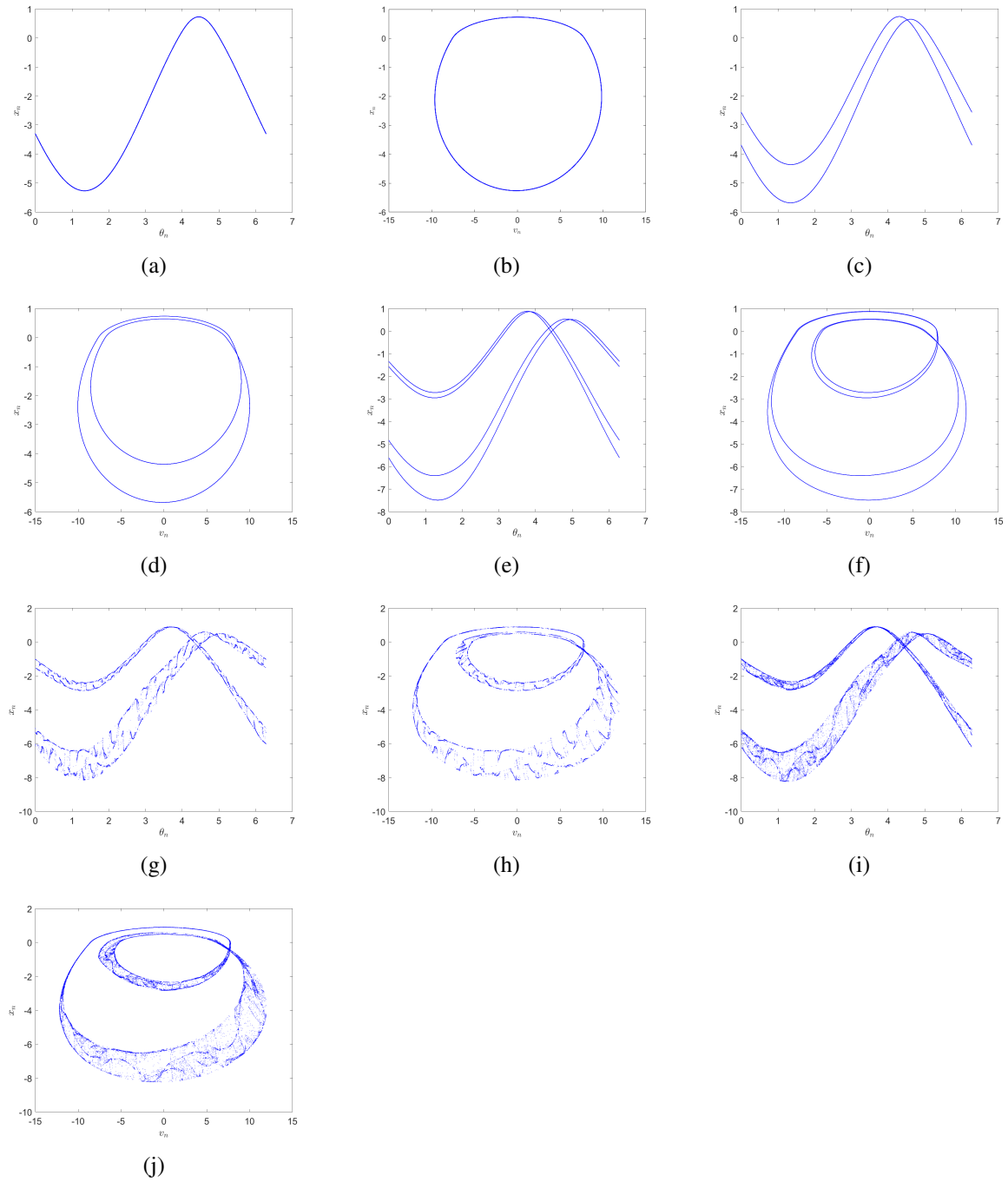

Figure 4: For $\varepsilon = 0.3$, the phase diagrams of attractors in the (θ_n, x_n)-plane and (v_n, x_n)-plane: (a), (b) $\omega = 3.45$, (c), (d)$\omega = 3.5$, (e), (f) $\omega = 3.551$, (g),(h) $\omega = 3.5647$, (i), (j) $\omega = 3.567$.

4.2. Check the strange properties of attractors

In the previous sections, we studied the evolution of the attractors with the help of phase diagram and power spectrum, and verified the nonchaotic characteristics of SNAs by the maximum

Lyapunov exponent. To further illustrate the strange properties of the attractor, we will use the phase sensitivity funtion, singular continuous spectrum and rational approximation method.

4.2.1. Phase sensitivity propety

If the attractor is regarded as a fractal curve, then its nondifferentiability can be detected by the phase sensitivity. This method is based on the sensitivity of the attractor to the phase of the external excitation. There are some special tangent bifurcation points in SNAs, where the derivative of these bifurcation points with respect to the phase is infinite, and the tangent is orthogonal to the θ-axis, showing that the attractor is nonsmooth. The derivative with respect to the external phase can be denoted as (c.f. [3])

$$S_i^N = \frac{\partial f_i}{\partial \theta} (i = 1, 2), \tag{7}$$

where N is the number of iterations. If S_i^N tends to be infinite as $N \to \infty$, the attractor is nonsmooth, which means that the attractor is strange.

The phase sensitivity can be calculated from the time series in the attractors. For any small ε, we can find n_0 to satisfy the phase difference $\varepsilon_0 = |\theta_{n_0} - \theta_0| < \varepsilon$, and the S_i^N can be approximately expressed as

$$S_i^N = \frac{\partial f_i}{\partial \theta} \approx \sum_{k=1}^{N-n_0} \left| \frac{f_i\left(k+n_0\right) - f_i(k)}{\theta\left(k+n_0\right) - \theta(k)} \right| = \sum_{k=1}^{N-n_0} \left| \frac{f_i\left(k+n_0\right) - f_i(k)}{\varepsilon_0} \right| (i = 1, 2), \tag{8}$$

where $k + n_0 \leqslant N$, and $f_i(k)$ denotes the kth iteration of f_i. The maximum value of S_i^N after N times iterations is denoted as

$$\tau_i^N = \max\left\{S_i^N\right\}. \tag{9}$$

If the number of iterations increases, the value of τ_i^N increases gradually. Then S_i^N tends to infinite as $N \to \infty$, which means that the attractor is strange.

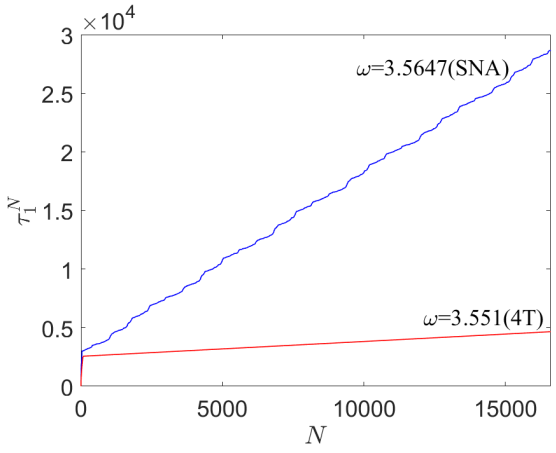

Figure 5: The phase sensitivity exponent τ_1^N versus N, the 4T for $\omega = 3.551$ (red line) and SNA for $\omega = 3.5647$ (blue line).

We take two groups of parameter values to verify strange properties by phase sensitivity function. Let $n_0 = 4182$, then $|\theta(k+n_0) - \theta(k)| \equiv 0.000672$, when $\omega = 3.5647$, the value of τ_1^N tends to infinity as the number of iterations increases, which indicates that the attractor is strange. On the contrary, when $\omega = 3.551$ the value of τ_1^N does not increase with the increase of iterations, which indicates that the attractor is smooth, see Fig. 5 .

4.2.2. Singular continuous spectrum

The strange properties of the attractor can be examined by means of the singular continuous spectrum. For $\omega = 3.5647$, the spectrum shows singular continuity (a fractal characteristic with multiple scale peaks), see Fig. 6(a). In general, $X(\Omega, T)$ and T have a power-law relationship, see [39] for details. Let

$$|X(\Omega, T)|^2 \sim T^{\rho}, \tag{10}$$

where ρ is a scaling exponent. If an SNA exists, then $1 < \rho < 2$. When the system exhibits periodic or quasiperiodic motion, the corresponding scaling exponent is $\rho = 2$. If the system exhibits chaotic motion, the scaling exponent is $\rho = 1$. For the SNA in Fig. 4(g), the corresponding finite-time Fourier spectrum $X(\Omega, T)$ versus T in logarithmic scale is exhibited in Fig. 6(b), where we detect a relatively robust power-law behavior with $\rho = 1.2564$. In addition, $X(\Omega, T)$ defines a path in a complex plane $(\mathrm{Re\,X}, \mathrm{Im\,X})$ when T is regarded as time and a fractal self-similar path corresponds to $|X(\Omega, T)|^2 \sim T^{1.2564}$, see Fig. 6(c).

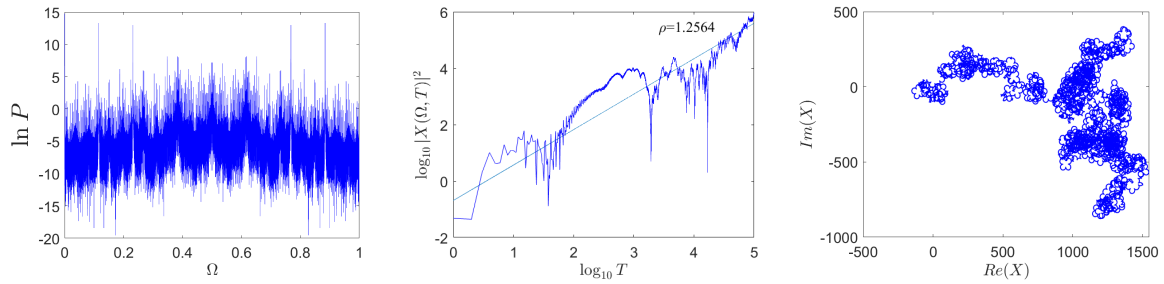

(a) (b) (c)

Figure 6: For $\omega = 3.5647$. (a) The singular continuous spectrum. (b) The finite-time Fourier spectrum $X(\Omega, T)$ versus T in logarithmic scale. (c) The fractal walk in the complex plane (ReX,ImX).

4.2.3. The rational approximation

The rational approximation is also an important method to determine the strange properties of SNAs, which is based on the fact that all irrational numbers can be approximated by appropriate rational numbers (c.f. [3]). In the following, we use rational numbers to approximate the frequency ξ, which is taken as $(\sqrt{5}-1)/2$. The ratio ξ_k of the Fibonacci sequences can be used to approximate ξ, where $\xi_k = F_{k-1}/F_k, F_k = F_{k-1} + F_{k-2}, F_1 = 1, F_2 = 1$, and $\xi = \lim_{k\to\infty} \xi_k$. Take the attractor in Fig. 4(j) as an example. The Figs. 7 are the phase diagrams of the attractor in the (θ_n, x_n)-plane for different approximate orders k. In Fig. 7(a), only some periodic points can be observed when $\xi_5 = 5/8$. As k gradually increases, the number of periodic points gradually increases, and the fractal characteristics of the attractor gradually

appear (Figs. 7(b) and (c)). When $\xi_{19} = 4181/6765$, the number of periodic points becomes virtually uncountable, the attractor begins to appear nonsmoothly, and an SNA emerges (Fig. 7(d)). We find that the higher is the order of the approximation, the more significant is the degree of the fractal structure of the attractor.

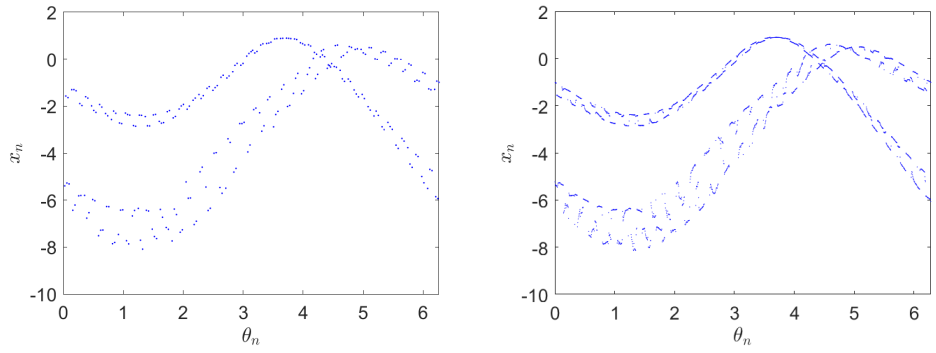

(a) $\xi_5 = 5/8$

(b) $\xi_{12} = 89/144$

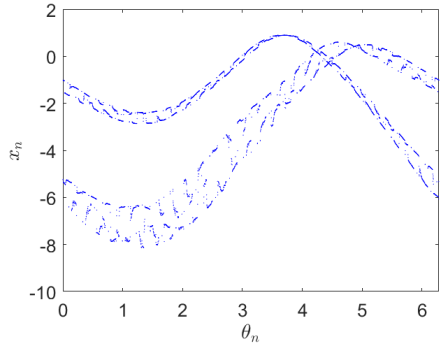

(c) $\xi_{17} = 1597/2584$

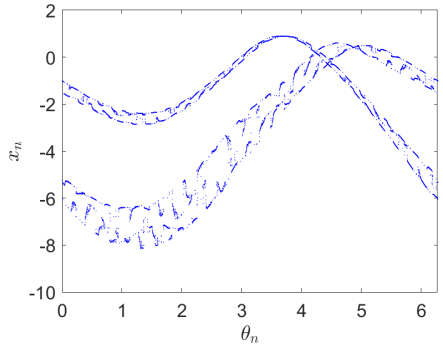

(d) $\xi_{19} = 4181/6765$

Figure 7: The rational approximations of the SNA for $\omega = 3.5647$ in the (θ_n, x_n)-plane.

4.3. The fractal route

In fractal routes for the creation of SNAs, a torus attractor gets increasingly wrinkled and transforms into an SNA without the apparent mediation of any nearby unstable orbit. This generation mechanism of SNAs is independent of bifurcation phenomenon.

We fix the parameter $\varepsilon = 3.1$ and let ω vary from 3.2 to 3.44. The other parameters and the initial values remain the same as Section 3.1. The attractors for successively larger ω are shown in Fig. 8. For $\omega = 3.2$, the attractor has one smooth branch, which indicates that the system is in a single torus state $(1\ \mathrm{T})$, see Fig. 8(b) below. As ω increases, the attractor does not undergo torus-doubling bifurcation as in the last scenario. Instead, the branch of the attractor becomes irregular as shown in Figs. 8(c) and (d), but the attractor is continuous. In other words, the system is still in a torus state for $\omega = 3.38$. When $\omega = 3.43$ the attractor becomes extremely wrinkled, and ultimately result is a strange attractor, see Figs. $8(\mathrm{e})$ and (f). Meanwhile, its maximum Lyapunov exponent is nonpositive ($\lambda \approx -0.00849$, see Fig. 9(a)). Therefore, it is

an SNA. For $\omega = 3.44$, the SNA is transformed into an attractor with a fractal structure and positive maximum Lyapunov exponent ($\lambda \approx 0.00458$), and thus the attractor (Fig. 8(g)) is chaotic.

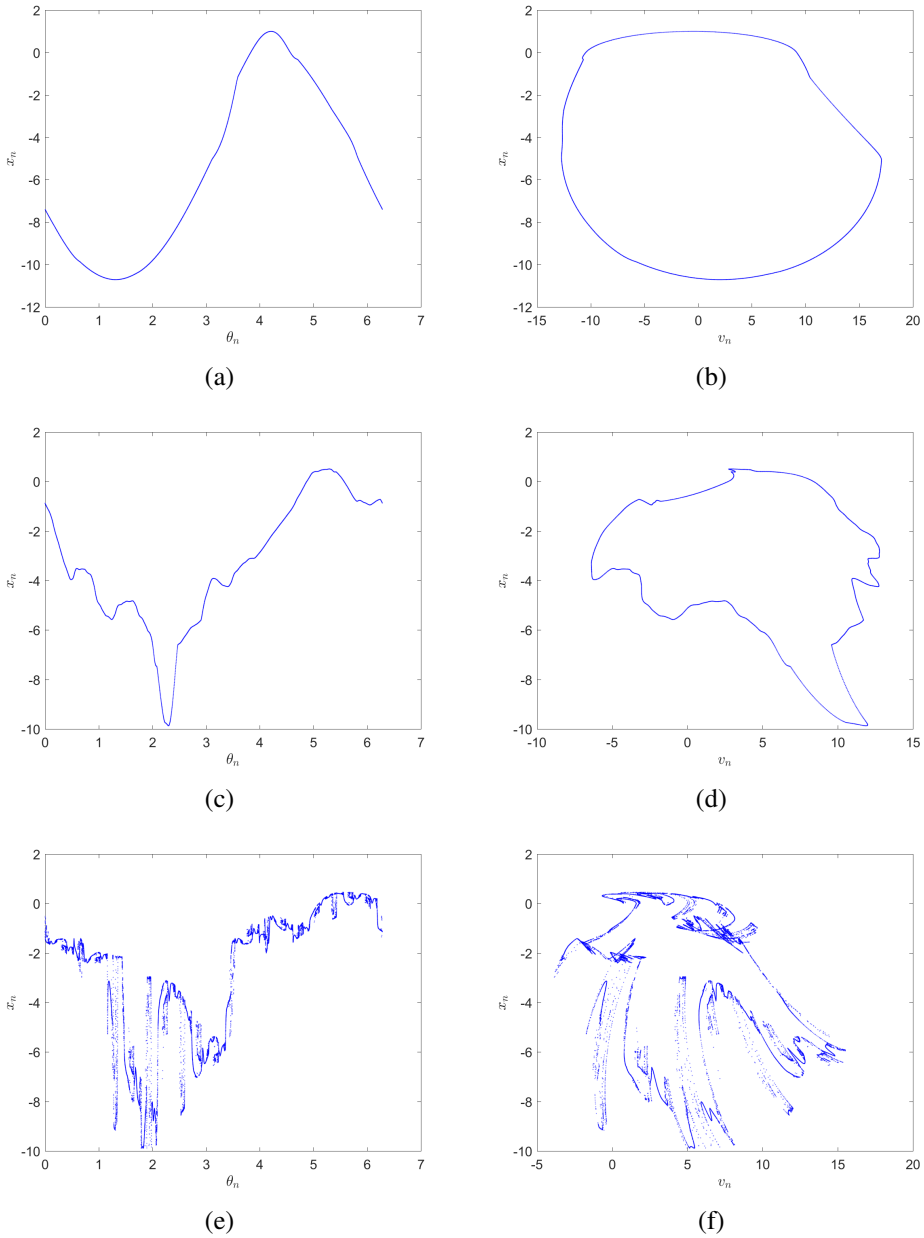

In the fractal route, it is sometimes difficult to decide when the transition to SNAs occurs, since the extremely wrinkled invariant curve looks very similar to an SNA. However, we can give a strict criterion by the phase sensitivity function. The Fig. 9(b) shows the time evolution of the maximum derivative, where the red and blue curves correspond to attractors as shown in Figs. 8(a) and (e), respectively. As the number of iterations increases, the derivative is not saturated after the transition to SNA, we infer that the derivative is not bounded. Therefore,

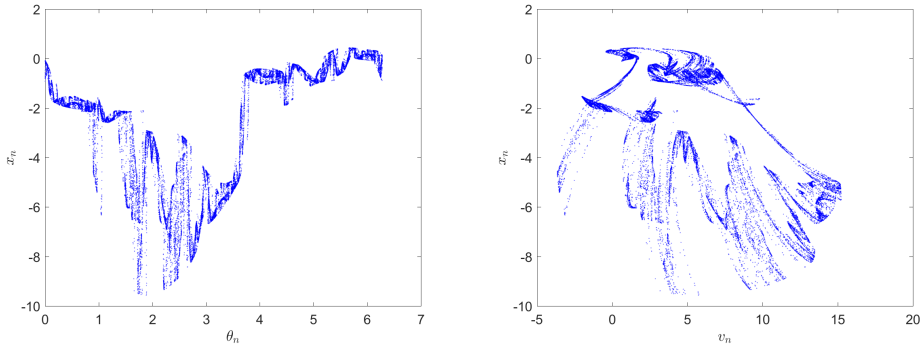

(g) (h)

Figure 8: For $\varepsilon = 3.1$, the phase diagrams of attractors in the (θ_n, x_n)-plane and (v_n, x_n)-plane:(a), (b)$\omega = 3.2$, (c), (d)$\omega = 3.38$, (e), (f) $\omega = 3.43$, (g), (h) $\omega = 3.44$.

the attractor shown in Fig. 8(e) is strange. To provide further evidence, the previous methods are also used to confirm the strange structure of SNA. We compute the scaling exponent ρ and present a reasonable power-law relationship $|X(\Omega, T)|^2 \sim T^{1.4540}$ and this behavior is shown in Fig. 9(c). Meanwhile, Fig. 9(d) demonstrates that the spectral trajectory in the complex plane (ReX, ImX) should exhibit a fractal behavior, as required for SNAs. To sum up, the attractor is an SNA.

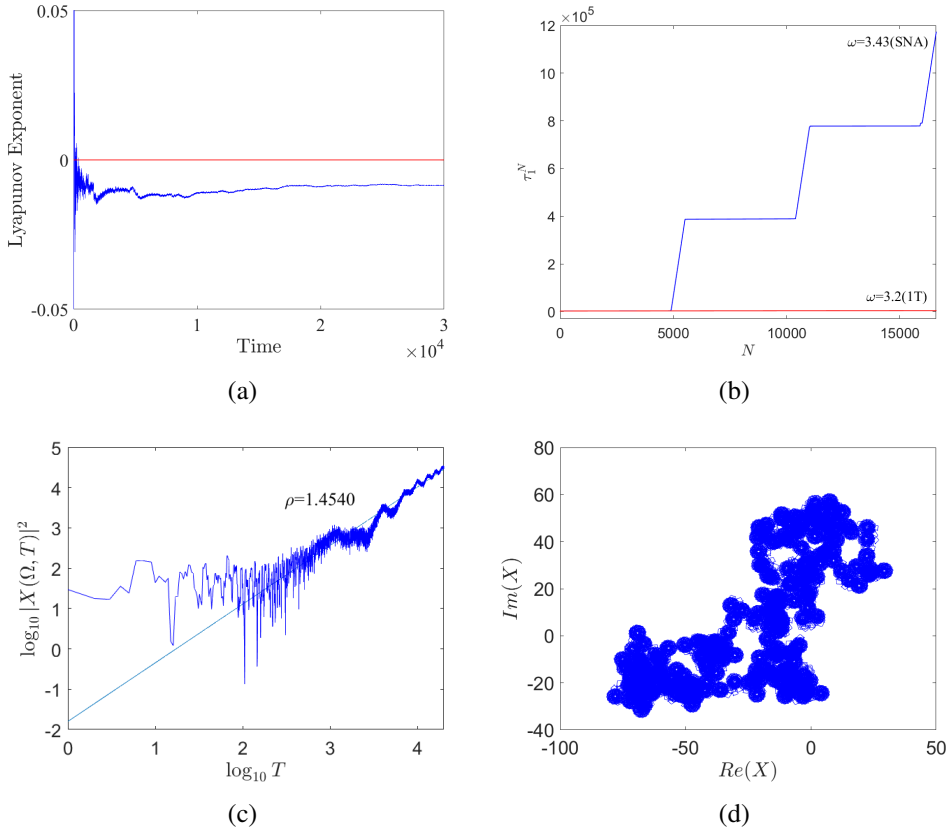

Figure 9: For $\omega = 3.43$. (a) The maximum Lyapunov exponent. (b) The phase sensitivity exponent τ_1^N versus N, the 1 T for $\omega = 3.2$ (red line) and SNA for $\omega = 3.43$ (blue line). (c) The finite-time Fourier spectrum $X(\Omega, T)$ versus T in logarithmic scale. (d) The fractal walk in the complex plane (ReX, ImX).

4.4. The bubbling route

In addition to the route studied above, we also identified an uncommon route in a piecewise linear oscillator, called bubbling route (c.f. [25, 26]) for the creation of SNAs. In this route, the torus quasiperiodic attractor forms local bubble like structures in some regions and wrinkling of these under external force. However, the rest of the strands of the torus outside the bubbles remain largely unaffected. It is worth noting that this route is quite different from the well known fractal route, where the entire strands of the n-period torus continuously deform and become extremely wrinkled as the control parameters change.

To illustrate the emergence of bubbling route to SNAs in the system (3), we fix the parameter $\varepsilon = 1.5$ and let the frequency ω vary from 3.36 to 3.37. The other parameters and the initial values remain the same as Section 3.1. For $\omega = 3.363$, a 1T quasiperiodic attractor (Figs. 10(a) and (b)) occurs. As ω is increased to 3.3645, in the 1T quasiperiodic attractor appears bubble-like structures in the strand of the torus, see Figs. 10(c) and (d). These bubble-like structures are localized, namely, they occur on partial regions of the torus while the remaining part of the torus strand remain unaffected. As ω increases further to 3.365, the bubbles deform and become extremely wrinkled, which lead to the formation of an SNA, see Figs. 10(e) and

(f). As ω continues to increase to 3.37, the SNA forms a 1-band chaotic attractor (Fig. 10(g)). This transition process from a quasiperiodic attractor to an SNA via the bubbling route can be further verified by the maximum Lyapunov exponent (Fig. 11(a)), phase sensitivity function (Fig. 11(b)), and singular continuous spectrum analysis (Fig. 11(c)): $\log_{10}|X(\Omega,T)|^2$ versus $\log_{10} T$, where $|X(\Omega,T)|^2 \sim T^{1.2286}$, and fractal trajectory in the complex plane (ReX, ImX) (Fig. 11(d)).

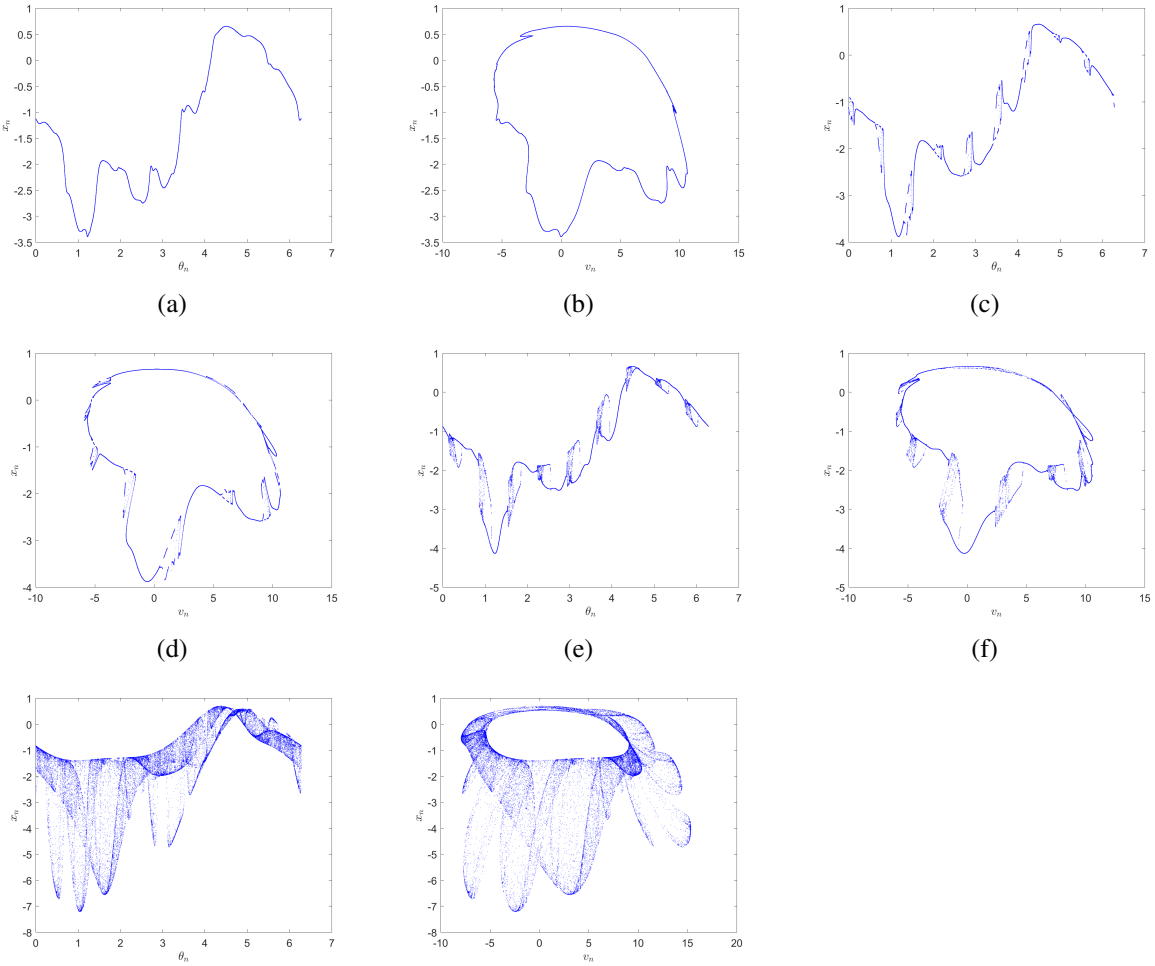

Figure 10: For $\varepsilon = 1.5$, the phase diagrams of attractors in the (θ_n, x_n)-plane and (v_n, x_n)-plane: (a), (b) $\omega = 3.363$, (c), (d)$\omega = 3.3645$, (e), (f) $\omega = 3.365$, (g), (h) $\omega = 3.37$.

The mechanism of the bubbling route is that the quasiperiodic orbit gets increasingly unstable in its transverse direction as the control parameter ω changes, resulting in the formation of the bubble-like structures. This is reflected in Fig. 10(e), in partial regions of the torus.

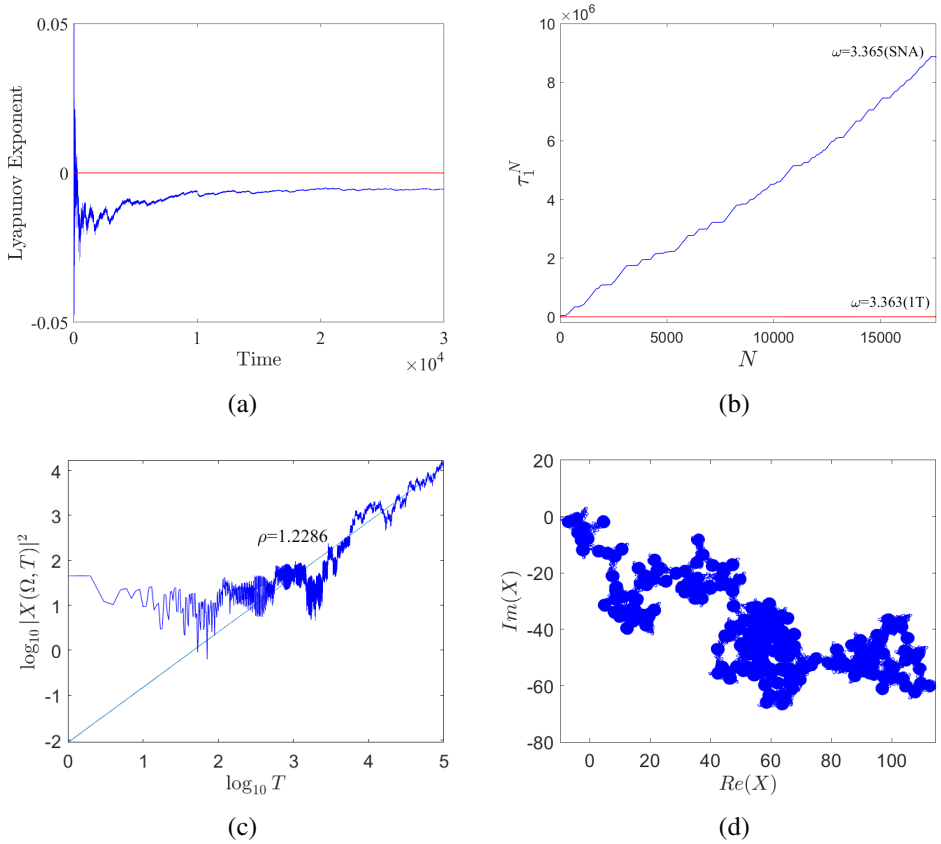

Figure 11: For $\omega = 3.365$. (a) The maximum Lyapunov exponent. (b) The phase sensitivity exponent τ_1^N versus N, the 1 T for $\omega = 3.363$ (red line) and SNA for $\omega = 3.365$ (blue line). (c) The finite-time Fourier spectrum $X(\Omega, T)$ versus T in logarithmic scale. (d) The fractal walk in the complex plane (ReX, ImX).

4.5. The type-I intermittency route

Intermittency routes can be the generation mechanisms for SNAs. We describe SNAs in terms of $4T$ torus intermittency, which is related to the saddle-node bifurcation. Let $\varepsilon = 0.1659095$ and the frequency ω vary from 9.995 to 10. For $\omega = 9.995$, the attractor is $4T$ quasiperiodic, as shown in Figs. 12 (a) and (b). When ω is increased to 10, the approximate shape of the quasiperiodic orbit of the system is still present, but there are many disordered points near the orbit, which are a characteristics of intermittency, as shown in Figs. 12 (c) and (d). Here the attractor is strange nonchaotic in Fig. 12 (c). The nonchaotic property is denoted by the maximum Lyapunov exponent $\lambda \approx -0.00161$ (Fig. 13(a)). The strange property of the attractor is characterized by the phase sensitivity (Fig. 13(b)) and the singular continuous spectrum (Fig. 13(c)).

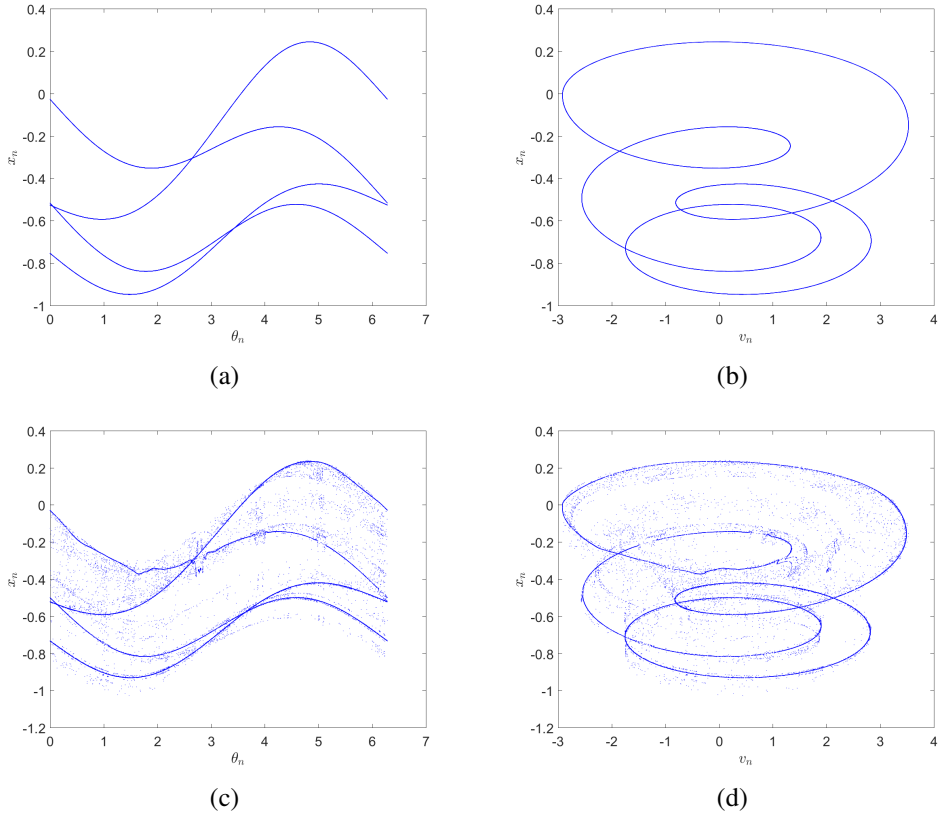

Figure 12: For $\varepsilon = 0.1659095$, the phase diagrams of attractors in the (θ_n, x_n)-plane and (v_n, x_n)-plane: (a), (b) $\omega = 9.995$, (c), (d)$\omega = 10$.

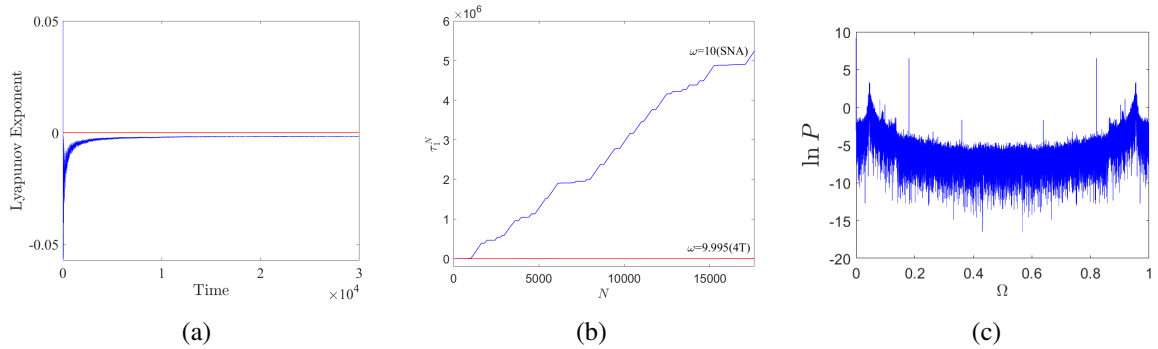

Figure 13: For $\omega = 10$. (a) The maximum Lyapunov exponent. (b) The phase sensitivity exponent τ_1^N versus N, the 4 T for $\omega = 9.995$ (red line) and SNA for $\omega = 10$ (blue line). (c) The singular continuous spectrum.

5. Conclusions

Most of the research on strange nonchaotic dynamics focuses on smooth systems in different fields. In this work, the dynamics of a single-degree-of-freedom nonlinear oscillator under

quasiperiodic excitation is considered. The complicated and interesting strange nonchaotic dynamics phenomena are revealed via the phase diagram, maximum Lyapunov exponent, singular continuous spectrum, phase sensitivity function, rational approximation, and so on. We demonstrate that the first scenario is torus-doubling bifurcation followed by the transition from the torus attractors to SNAs in such class of nonsmooth systems. The second is that the torus does not undergo period-doubling cascade as controlling parameters vary, instead, the torus becomes extremely wrinkled, loses smoothness and finally becomes fractal. The third is that the quasiperiodic attractor gets increasingly unstable in its transverse direction as the control parameter changes, resulting in the formation of bubble-like structures in partial regions of the torus, which eventually evolves into an SNA. The last one is that in the neighborhood of a saddle-node bifurcation many disordered points abruptly appear during the transition from $4T$ torus to SNA. The results of this work offer ideas for the study of strange nonchaotic dynamics in nonsmooth systems, as well as provide support for the design and optimization of devices in engineering fields.

Acknowledgments

We sincerely thank the people who give valuable comments. The paper is supported by the National Natural Science Foundation of China (No. 12172306), the "Double-First Class" Major Research Programs, Educational Department of Gansu Province (No. GSSYLXM-04), the Innovation Fund Project of Colleges and Universities in Gansu Province (No. 2021A-040).

References

[1] Grebogi C., Ott E., Pelikan S., Yorke J. A. [1984] "Strange attractors that are not chaotic," Physica D **13**, 261-268.

[2] Ding M., Grebogi C., Ott E. [1989] "Evolution of attractors in quasiperiodically forced systems: from quasiperiodic to strange nonchaotic to chaotic," Physical Review A **39**, 2593-2598.

[3] Pikovsky A. S., Feudel U. [1995] "Characterizing strange nonchaotic attractors," Chaos **5**, 253-260.

[4] Nishikawa T., Kaneko K. [1996] "Fractalization of a torus as a strange nonchaotic attractor," Physical Review E **54**, 6114-6124.

[5] Ditto W. L., Spano M. L., Savage H. T., Rauseo S. N., Heagy J., Ott E. [1990] "Experimental observation of a strange nonchaotic attractor," Physical Review Letters **65**, 533.

[6] Thamilmaran K., Senthilkumar D. V., Venkatesan A., Lakshmanan M. [2006] "Experimental realization of strange nonchaotic attractors in a quasiperiodically forced electronic circuit," Physical Review E **74**, 036205.

[7] Lindner J. F., Kohar V., Kia, B., Hippke M., Learned J. G., Ditto W. L. [2015] "Strange Nonchaotic Stars," Physical Review Letters **114**, 054-101.

[8] Glendinning P. [2002] "Global attractors of pinched skew products," Dynamical Systems **17**, 287-294.

[9] Stark J. [2003] "Transitive sets for quasi-periodically forced monotone maps," Dynamical Systems **18**, 351-364.

[10] Glendinning P., Jäeger T., Keller G. [2006] "How chaotic are strange nonchaotic attractors," Nonlinearity **19**, 2005-2022.

[11] Keller G. [1996] "A note on strange nonchaotic attractors," Fundamenta Mathematicae **151**, 139-148.

[12] Ding M., Grebogi C., Ott E. [1989] "Dimensions of strange nonchaotic attractors," Physics Letters A **137**, 167-172.

[13] Fuhrmann G., Gröger M., Jäger T. [2018] "Non-smooth saddle-node bifurcations II: Dimensions of strange attractors," Ergodic Theory and Dynamical Systems **30**, 2989-3011.

[14] Haro À., Puig J. [2006] "Strange nonchaotic attractors in Harper maps," Chaos **16**, 033127.

[15] Romeiras F. J., Ott E. [1987] "Strange nonchaotic attractors of the damped pendulum with quasiperiodic forcing," Physical Review A **35**, 4404-4413.

[16] Prasad A., Negi S. S., Ramaswamy R. [2001] "Strange nonchaotic attractors," International Journal of Bifurcation and Chaos **11**, 291–309.

[17] Feudel U., Kuznetsov S., Pikovsky A. S. [2006] "Strange Nonchaotic Attractors: Dynamics between Order and Chaos in Quasiperiodically Forced Systems," World Scientific Publishing Co. Pte. Ltd., Singapore., Chapter 6, pp. 75-127.

[18] Li G., Yue Y., Xie J., Grebogi C. [2019] "Strange nonchaotic attractors in a nonsmooth dynamical system," Communications in Nonlinear Science and Numerical Simulation **78**, 104858.

[19] Heagy J. F., Hammel S. M. [1994] "The birth of strange nonchaotic attractors," Physica D **70**, 140-153.

[20] Zhang Y., Luo G. [2013] "Torus-doubling bifurcations and strange nonchaotic attractors in a vibro-impact system," Journal of Sound and Vibration **332**, 5462-5475.

[21] Datta S., Ramaswamy R., Prasad A. [2004] "Fractalization route to strange nonchaotic dynamics," Physical Review E **70**, 046203.

[22] Prasad A., Mehra V., Ramaswamy R. [1997] "Intermittency Route to Strange Nonchaotic Attractors," Physical Review Letters **79**, 4127-4130.

[23] Kim S. Y., Lim W., Ott E. [2013] "Mechanism for the intermittent route to strange nonchaotic attractors," Physical Review E **67**, 056203.

[24] Yalçınkaya T., Lai Y. C. [1996] "Blowout bifurcation route to strange nonchaotic attractors," Physical Review Letters **77**, 5039-5042.

[25] Senthilkumar D. V., Srinivasan V., Thamilmaran K., Lakshmanan M. [2008] "Birth of strange nonchaotic attractors through formation and merging of bubbles in a quasiperiodically forced Chua's oscillator," Physical Review E **78**, 066211.

[26] Suresh K., Prasad A., Thamilmaran K. [2013] "Bubbling route to strange nonchaotic attractor in a nonlinear series LCR circuit with a nonsinusoidal force," Physics Letters A **377**, 612–621.

[27] Li G., Yue Y., Grebogi C., Li D., Xie J. [2022] "Strange nonchaotic attractors in a quasiperiodically forced piecewise linear system with noise," Fractals **30**, 2250003.

[28] Yue Y., Miao P., Xie J. [2017] "Coexistence of strange nonchaotic attractors and a special mixed attractor caused by a new intermittency in a periodically driven vibro-impact system," Nonlinear Dynamics **87**, 1-21.

[29] Cheng T., Zhang Y., Shen Y. [2021] "Infinite number of parameter regions with fractal nonchaotic attractors in a piecewise map," Fractals **29**, 2150087.

[30] Li G., Yue Y., Xie J., Grebogi C. [2020] "Multistability in a quasiperiodically forced piecewise smooth dynamical system," Communications in Nonlinear Science and Numerical Simulation **84**, 105165.

[31] Shen Y., Zhang Y. [2019] "Mechanisms of strange nonchaotic attractors in a nonsmooth system with border-collision bifurcations," Nonlinear Dynamics **96**, 1405–1428.

[32] Zhang Y., Shen Y. [2020] "A New Route to Strange Nonchaotic Attractors in an Interval Map," International Journal of Bifurcation and Chaos **30**, 2050063.

[33] Li G., Yue Y., Grebogi C., Li D., Xie J. [2021] "Strange nonchaotic attractors and multistability in a two-degree-of-freedom quasiperiodically forced vibro-impact system," Fractals **29**, 2150103.

[34] Liu Y., Wang Q., Xu H. [2017] "Bifurcations of periodic motion in a three-degree-of-freedom vibro-impact system with clearance," Communications in Nonlinear Science and Numerical Simulation **48**, 1-17.

[35] Kundu S., Banerjee S., Ing J., Pavlovskaia E., Wiercigroch M. [2012] "Singularities in soft-impacting systems," Physica D **241**, 553-565.

[36] Aguiar R. R., Weber H. I. [2011] "Mathematical modeling and experimental investigation of an embedded vibro-impact system," Nonlinear Dynamics **65**, 317–334.

[37] Pikovsky A. S., Feudel U. [1994] "Correlations and spectra of strange non-chaotic attractors," Journal of Physics A **27**, 5209–5219.

[38] Nayfeh A. H., Balachandran B. [1995] "Applied Nonlinear Dynamics," John Wiley & Sons, Inc., New York.

[39] Aravindh S. M., Venkatesan A., Lakshmanan M. [2018] "Strange nonchaotic attractors for computation," Physical Review E **97**, 052212.